Hybrid Motion Simulator for Capturing H-II Transfer Vehicle by Flexible Space Manipulator

Ippei Takahashi*, Satoko Abiko*, Xin Jiang*, Teppei Tsujita*, Masaru Uchiyama*
Hiroki Nakanishi⋆, Hiroshi Ueno◇, and Mitsushige Oda⋆ ◇

*Tohoku University, Japan
e-mail : {ippei, abiko, jiangxin, tsujita, uchiyama}@space.mech.tohoku.ac.jp

⋆Tokyo Institute of Technology, Japan
e-mail : nakanishi.hiroki@mes.titech.ac.jp, oda.m.ab@m.titech.ac.jp

◇Japan Aerospace Exploration Agency (JAXA), Japan
e-mail : ueno.hiroshi@jaxa.jp

Abstract

This paper presents development of a dynamic motion simulator for orbital missions to transfer H-II Transfer Vehicle (HTV) to the International Space Station (ISS) based on hybrid motion simulator. In the missions, the end effector which is a type of snare wires is used as a grasping mechanism. This capturing method is known as a safer and more reliable method in space. It is expected that this method is adopted in future orbital missions. However, it is still necessary to ensure and analyze the safe capturing operation in advance. Therefore, the simulation on ground is definitely required for not only behavior analysis of the capturing the orbital target but also suggestion of methods for avoiding accidental troubles. The paper presents a hybrid motion simulator for the mission to capture the HTV. The simulator is developed with half-scaled model by following the similarity rule. Then we discuss the effect of time delay and stability which are general problems of the hybrid motion simulator. With the developed system, several case studies are carried out for capturing the HTV.

1 Introduction

The International Space Station (ISS) is a symbol of the contemporary space development. Various space experiments are executed on the ISS to obtain new knowledge and skills under the microgravity environment. Basically, over three astronauts always stay at the ISS, and they execute these experiments. Therefore, it is essential to regularly transfer the cargo of daily necessities to the ISS. Currently, the H-II Transfer Vehicle (HTV) is used as one of the methods for achieving this task (Fig. 1). The HTV missions have already succeeded four times, and it is planned to continue launching the HTV. Here, safety is the most important to execute the manned space mission. If the difficult or new missions are executed on orbit, the evaluation of those missions is needed before launching.

Figure 1. HTV ©JAXA

Under such a background, we have collaborated with Japan Aerospace Exploration Agency (JAXA) to construct a high-precision simulator on the ground for capturing and berthing a massive payload by orbital robotic manipulator. This paper presents a part of this collaborated research. The paper focuses on development of Hybrid Motion Simulator (HMS) for capturing the HTV by the Space Station Remote Manipulator System (SSRMS).

The capture method in Fig. 2 is used in the HTV mission. A Latching End Effector (LEE) mounted on the tip of a space manipulator and a Grapple Fixture (GF) mounted on the HTV are used as capture mechanism. The capture method with the LEE and GF is safe and reliable because the GF shaft is captured inside enclosed region made by three snare wires mounted on the LEE. In this research, this method is called “capture in enclosed region”. Additionally, there is an advantage that it is not required to precisely align the center of LEE and the GF shaft. Therefore, this capture method is expected to be used in various orbital operations.

On the other hand, it is very difficult to model the

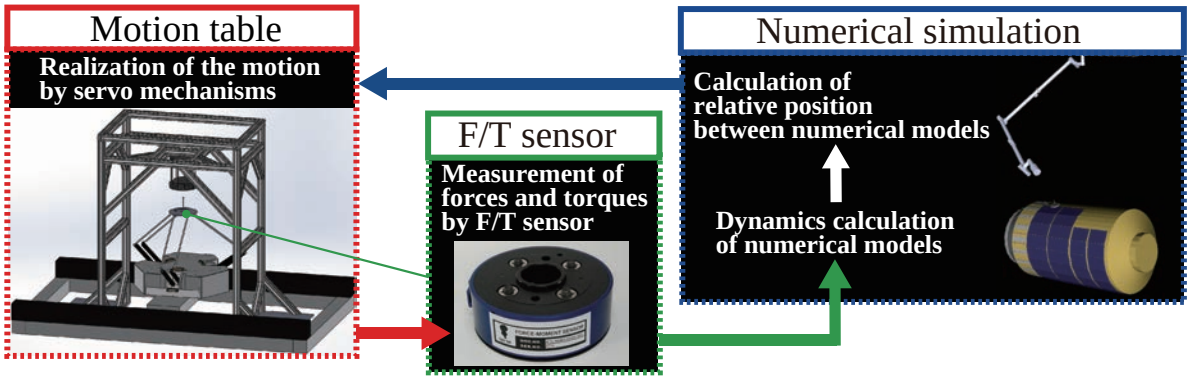

Figure 3. Concept of Hybrid motion simulator

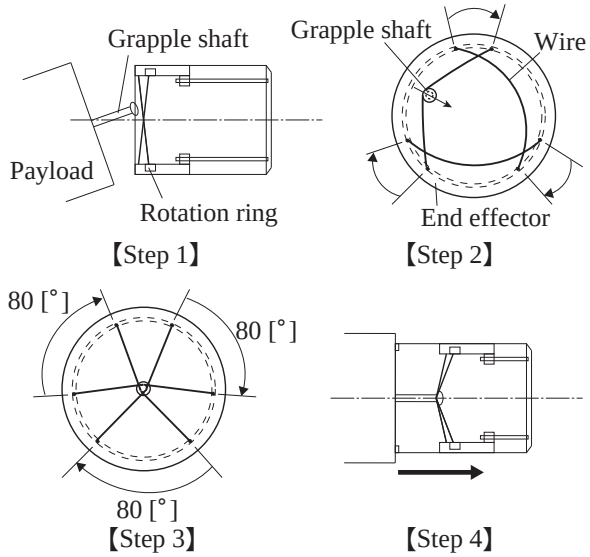

Figure 2. Sequence of HTV mission ©JAXA

snare wire in numerical simulator. Some researchers have tried modeling the snare wire by executing contact experiment [2][3]. However the derived wire model is not versatile due to limited experimental conditions. Therefore, we use the HMS which does not require the modeling of the snare wire because the part suffering from contact is replaced with a part of hardware in the HMS. Then, the HMS is capable of executing the simulation based on real contact phenomenon.

In order to develop the HMS for the HTV mission, it is required to discuss two problems. One is to derive the law of similarity between the simulation and real model because the scale of HMS is limited. The other is to verify how much delay time affects the result of the simulation for capturing the HTV. This paper discusses above two problems, and then describes the simulation results of the HTV capture.

2 System Configuration of HMS for Capturing HTV

2.1 Hybrid Motion Simulator

The HMS is a numerical simulator which embeds hardware experiment in the loop. It can simulate three-dimensional relative motion between two objects, such as a space robot and a floating target, under microgravity environment on the ground. It is generally difficult to develop a precise model of complex phenomena such as multi contacts or impacts in the numerical simulation. This problem is resolved by replacing the parts where physical contact occurs to the parts of hardware.
The hardware suffering from contact is called “physical model”, and the model constructed in the numerical simulation is called “numerical model” in this paper. The concept of the HMS is shown in Fig. 3 and the process of the simulation is as follows:

1. Measure forces and torques exerted on the physical model by using the force/torque sensor,
2. Send the observed forces and torques to the corresponding numerical models in numerical simulation,
3. Calculate the dynamics of whole systems such as the space robot and the target in the numerical simulation,
4. Demonstrate the relative motion of the systems by servo mechanisms of the HMS in real time.

The simulation is executed by repeating from step 1 to step 4.

2.2 Physical Model

In the HTV capturing simulator, we developed two fundamental physical models. One is a Grapple Fixture (GF) and the other is a Latching End Effector (LEE).

2.2.1 Grapple Fixture

The GF is a captured mechanism mounted on an orbital target such as the HTV and grappled by a space manipulator. The developed GF physical model is shown in

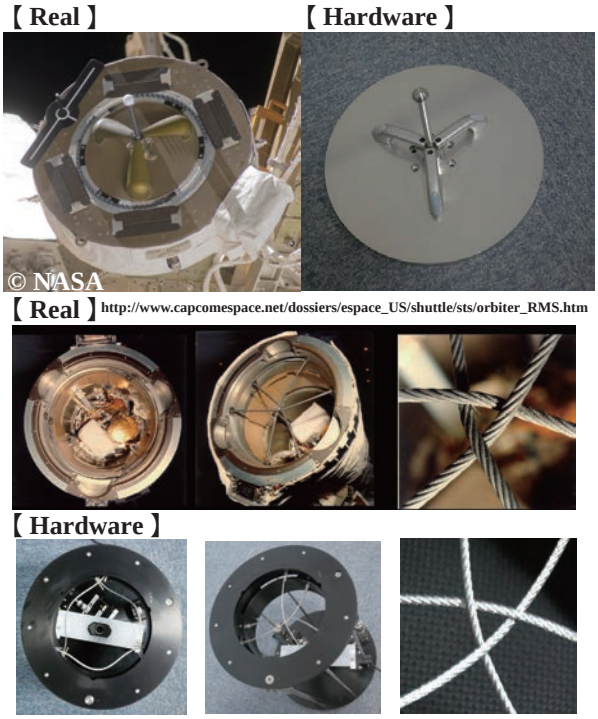

Figure 4. Comparison between the developed hardware and real mechanisms

Fig. 4. The GF consists of a grapple shaft captured by the LEE and three Grapple Cam Arms used as a guide in docking with the LEE.

2.2.2 Latching End Effector

The LEE is a capturing mechanism mounted on the tip of the Space Station Remote Manipulator System (SSRMS) or Shuttle Remote Manipulator System (SRMS). The LEE has capabilities to grapple the GF shaft inside the enclosed region formed by three snare wires and to drag the GF into the LEE housing to firmly fix the GF on the LEE. A sequence of the capture with the above two mechanisms is as follows (Fig. 2):

1. The LEE approaches the GF, and the GF shaft is inserted into the enclosed area formed by three snare wires on the LEE,
2. After the shaft is inserted, the snare wires move to make the enclosed area smaller to confine the GF shaft in the center of the LEE,
3. A ring on which one end of each wire is connected inside the LEE housing is dragged into the LEE, and the LEE and the GF are contacted completely.

According to this sequence, the LEE model needs to have following two functions :

- Rotating the ring to keep the GF shaft inside the enclosed region formed by the snare wires,
- Pulling the ring into the LEE housing to firmly fix the GF shaft.

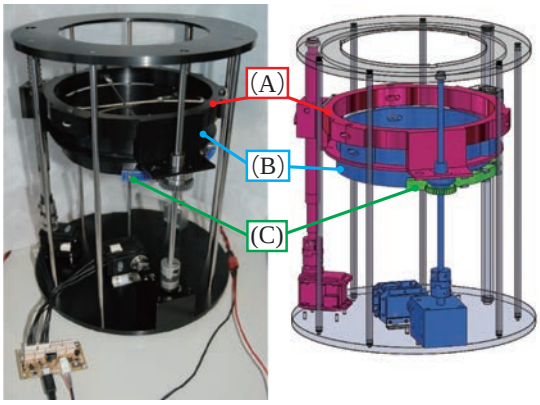

Figure 5. Overview of LEE mockup

Table 1. Main parameters of physical and numerical models

	Real size		Half-scaled size	
Physical model	LEE	GF	LEE	GF
Height [mm]	–	287	293	141
Diameter [mm]	–	572	150 (Hole)	250
Mass [kg]	243.66	59.4	3.9	1.6
Numerical model	SSRMS	HTV	SSRMS	HTV
Length [m]	17.6	10	8.8	5
Diameter [m]	0.35	4.4	0.175	2.2
Mass [kg]	1800	16000	225	2000

Fig. 5 shows the developed LEE model comprising above two functions. The first function was achieved by using a rack and pinion, and a motor. The motor rotates a rack and pinion attached the blue-colored ring part (B) in the figure. One end of the wire is fixed to the pink-colored ring part (A) and the other end is fixed to the blue-colored ring part (B) in the figure. Therefore, when the blue-colored ring is rotated, the wires close the enclosed area to confine the GF shaft. The second function was constructed by using a ball screw. The two ring parts are moved by the ball screw attached to the motor.

The specifications of two physical models are shown in Table 1.

2.3 Numerical Model

The main parameters of numerical models are shown in Table 1. The detail parameters of the SSRMS in the numerical model are quoted from the reference [5]. Space manipulators such as SRMS and SSRMS are known as flexible joint manipulators [6]. The PD control is applied in order to simulate the joint characteristics of the SSRMS in the HMS. This control is simply expressed as follows :

$$\boldsymbol{\tau} = \boldsymbol{K}_{\mathrm{p}} \left(\boldsymbol{q}_{\mathrm{ref}} - \boldsymbol{q}_{\mathrm{cur}} \right) - \boldsymbol{K}_{\mathrm{d}} \, \dot{\boldsymbol{q}}_{\mathrm{cur}} \tag{1}$$

where $\boldsymbol{\tau}$ is the joint torque, and $\boldsymbol{q}_{\mathrm{ref}}$, $\boldsymbol{q}_{\mathrm{cur}}$ and $\dot{\boldsymbol{q}}_{\mathrm{cur}}$ are desired joint angle, measured joint angle and measured joint angular velocity, respectively. $\boldsymbol{K}_{\mathrm{p}}$ and $\boldsymbol{K}_{\mathrm{d}}$ are stiffness and damping matrices of each joint. The stiffness of the joint has nonlinearity as mentioned in the reference [5]. Therefore, K_{p} is determined as nonlinear characteristic.

In the real operation, the control mode of SSRMS is switched to the velocity control mode called "LIMP mode" when the HTV is captured by the SSRMS. In this mode, the joint characteristic is expressed as follows :

$$\boldsymbol{\tau} = \boldsymbol{K}_{\mathrm{v}} \left(\dot{\boldsymbol{q}}_{\mathrm{ref}} - \dot{\boldsymbol{q}}_{\mathrm{cur}} \right) \tag{2}$$

where $\boldsymbol{K}_{\mathrm{v}}$ is the velocity gain matrix. This mode is used in the HTV capturing simulation.

On the other hand, the HTV was modeled as one rigid body in this study. The GF was attached at a point distant from the center of mass in common with real one. Therefore, the attitude of the HTV is greatly changed when the GF receives large external forces.

The CG of the SSRMS, HTV and ISS are constructed in order to check the motion of models visually.

3 Law of Similarity Between Real Model and Numerical Model of HTV and SSRMS

3.1 Derivation of Similarity Rule

Two parts of hardware for the LEE and GF developed in this study were scaled down by half size of real ones. Accordingly, the numerical models of the SSRMS and HTV are also scaled down by half size of real ones. Then, the similarity rule between the real and half models is necessary to obtain corresponding behavior between them. Regarding the HTV, its mass and moment of inertia are simply scaled down to $1/2^3$, $1/2^5$, respectively because the HTV is modeled as one rigid body. As for the SSRMS, the joint characteristics of the SSRMS must be properly scaled down with the law of similarity. Therefore, we derived a law of similarity to solve the problem [7]. To demonstrate the similarity rule for the SSRMS, let us consider a simple articulated system which has 1 link connected with a fixed base with 1 rotational joint. The joint has flexibility and viscous damping factor. The equation of motion of this model is expressed as follows :

$$\tau = I\ddot{q}(t) + d\dot{q}(t) + k\Delta q(t) \tag{3}$$

where $\boldsymbol{\tau}$ is the joint torque, and $\boldsymbol{q}$ is joint angle. I denotes moment of inertia. d and k represent coefficients of viscous damping and stiffness respectively. Time t is an independent variable in Eq. (3). Here, to obtain non-dimensional equation, let us determine representative time T, representative angle Q and representative torque S as representative quantities and non-dimensional time t^*, non-dimensional angle q^* and non-dimensional torque τ^* as dimensionless quantities. Then, t, q and τ in Eq. (3) are expressed as $t = Tt^*, q = Qq^*, \tau = S\tau^*$. These parameters are substituted for Eq. (3), and Eq. (3) is simplified as follows :

$$\frac{ST^2}{IQ}\tau^* = \ddot{q}^* + d\frac{T}{I}\dot{q}^* + \frac{kT^2}{I}\Delta q^* \tag{4}$$

Under the assumption that the coefficient of the third term of right side in Eq. (4) is 1, the representative time T is determined as $T = \sqrt{I/k}$. With this assumption, Eq. (4) is expressed as follows :

$$\frac{S}{kQ}\tau^* = \ddot{q}^* + \frac{d}{\sqrt{kI}}\dot{q}^* + \Delta q^* \tag{5}$$

It is assumed that the coefficient of the left side in Eq. (5) is 1, and then the representative torque S is determined as $S = kQ$. Accordingly, Eq. (5) is expressed as the following non-dimensional equation.

$$\tau^* = \ddot{q}^* + 2\zeta\dot{q}^* + \Delta q^* \tag{6}$$

where $\zeta = d/2\sqrt{kI}$. Among the parameters of real and half-scaled models, mass and length of both models, joint stiffness k and joint viscous damping d of real model are known. Therefore, it is required to derive the joint stiffness k', joint viscous damping d' and joint torque τ' of half-scaled model by using the above non-dimensional equation. Here, we assume that the representative time T' of the half-scaled model equals to the representative time T of real one. Then, the joint stiffness k' becomes $k' = k/32$ because of $I' = I/32$ and $T = \sqrt{I/k}$.

Next, it is clear that Eq. (6) depends on damping ratio ζ. $\zeta = d/2\sqrt{kI}$ in the real and half-scaled models must be equal to each other in order to express corresponding dynamics behavior. Then, the viscous damping d' in the half-scaled model is obtained as follows:

$$\zeta = \frac{d}{2\sqrt{kI}} = \zeta' = \frac{d'}{2\sqrt{k'I'}} \Leftrightarrow d' = \sqrt{\frac{k'I'}{kI}}d = \frac{d}{32} \tag{7}$$

Finally, the representative torque is expressed by using the parameters of half-scaled model as follows :

$$S' = k'Q' \Leftrightarrow S' = \frac{k}{32}Q' \tag{8}$$

Here, if the joint angle of half-scaled model q' is equal to that of real one q, the representative angle of half model Q' is equal to that of real one Q. In this case, representative torque of half model is equal to $S/32$. From the above, the torque of half-scaled model τ' is expressed as follows :

$$\tau^* = \frac{\tau}{S} = \frac{\tau'}{S'} \quad \Leftrightarrow \quad \tau' = \frac{\tau}{32} \tag{9}$$

where the representative torque S' of the half-scaled model is expressed as $S' = k'Q' \leftrightarrow S' = kQ'/32$ and $q' = q$, $Q' = Q$.

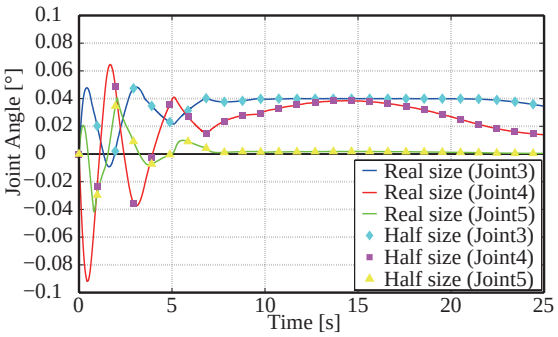

Figure 6. Results of joint angle behavior of SSRMS

3.2 Verification of Similarity Rule

The above mentioned similarity rule can be easily applied to a multi-DOF articulated body system with rotational joints as the SSRMS. The simulation of the SSRMS model was executed in order to verify the similarity rule derived in section 3.1. The joint behavior of the half-scaled model was compared with the joint behavior of the real model at Joint 3, 4, 5 in the case inputting the pulse as the initial torque into Joint 3. The torque given to joint 3 of half-scaled model is 1/32 torque of real model.

The variations of joint angles at Joint 3, 4, 5 are shown in Fig. 6. In this rule, it is assumed that the joint angle q' of half-scaled model is equal to the joint angle q of real one. These results show that the similarity rule is valid because the joint behaviors of real and half-scaled model agreed with each other.

4 Delay Time of HMS

Delay time is the most important problem of hybrid motion simulator in common. This problem can be observed, in the worst case, as the coefficient of restitution (COR) greater than 1 in contact hybrid motion simulator. This is because the system energy increases due to delay time induced by the servo delay of robotic motion system and sampling time etc. Delay time compensation has been proposed to solve this problem[8] and is applied to the HMS developed in our laboratory. However the compensation lacks versatility because it needs to know the COR of real phenomenon in advance.

On the other hand, it is known that the influence of dead time decreases as the contact period increases in the contact between two objects. The contact duration becomes longer when the objects subjected to contact are flexible or their mass and moment of inertia are relatively large. The grasping mechanism with the LEE and GF uses flexible snare wires. Therefore, the contact phenomenon between the LEE and the GF in the HMS seems to be stable. In this section, we evaluate the influence of the delay time in the contact between the snare wire and GF shaft in the HMS.

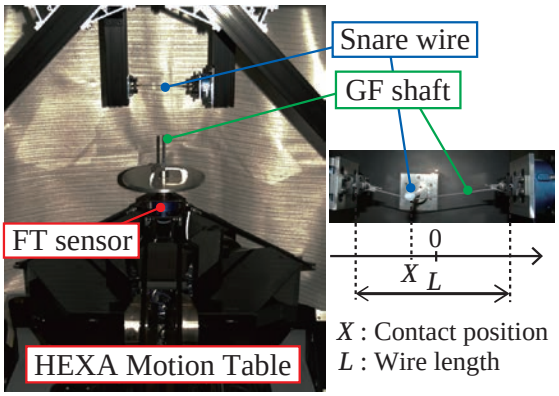

Figure 7. Contact Parameters

4.1 Experimental Condition

The experiment was carried out in one dimension. One snare wire was fixed with both ends on a fixed frame. A Force/Torque (F/T) sensor was attached on one end of the wire to measure the tension of the wire. The distance between two ends was adjustable. Therefore, conditions of the wire, e.g. tense wire or loose wire, could be arbitrarily set. The GF was mounted on the tip of the robotic motion table in the contact experiment with the HMS. One F/T sensor was attached on the bottom of the GF shaft to measure the reaction force due to the contact with the snare wire. An overview of the experiment system is shown in Fig. 7.

The total length of the snare wire was 180 [mm]. The GF shaft contacted with five contact positions of the snare wire. For each point, 5 trials were executed at the two patterns of the flexure (ΔL = 0, 10 [mm]). The mass of the half-scaled HTV model was 2000 [kg], and the contact velocity was 1 [mm/s].

4.2 Experimental Results and Discussion

This section discusses the stability of the HMS from the aspect of the frequency of the contact dynamics and the COR. An experiment where a rigid body contacted with a stiff wall was executed in our laboratory. In the experiment, we analyzed frequency of the contact dynamics under the assumption that the contact dynamics was modeled as a liner mass-spring-damper system. In such model, the contact frequency f_c is represented as follows :

$$f_c = \frac{1}{2\pi}\sqrt{\frac{K}{M}} \tag{10}$$

where K is the whole system stiffness, and M is the mass of contact object. From the frequency analysis, the simulation in the HMS is stable when the system frequency is lower than 0.398 [Hz]. This indicates that the whole system stiffness K under 12500 [N/m] provides the stable system for contact hybrid motion simulation with the object whose mass is 2000 [kg]. Fig. 8 shows the experimental

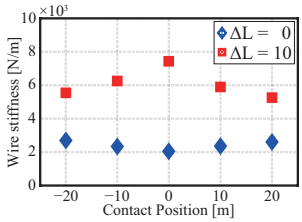

Figure 8. Wire stiffness

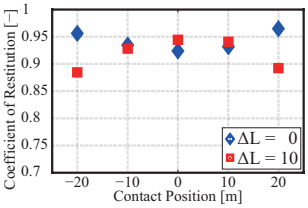

Figure 9. COR

results about the contact stiffness between the snare wire and the GF shaft. The experiment was carried out under two conditions of the snare wire, namely flexure of the wire $\Delta L = 0$ and 10 [mm]. It was observed from the result that the stiffness in the both conditions satisfied the criterion for stable HMS.

From the aspect of the COR, Fig. 9 shows the experimental results about the COR. Although the shape of graph of the COR between the flexure $\Delta L = 0$ and 10 [mm] were different, it was confirmed that the contact simulation in each condition was stable because the COR of each condition was lower than 1.

Therefore, the HMS has enough capability for the HTV capture.

5 Simulation for Capturing HTV

The simulation of capturing the HTV was executed by using the HMS constructed in this research. In this paper, we only consider the sequence from step 2 to step 3 in Fig. 2. The behavior of the HTV and SSRMS on the real flight missions were analyzed in the reference [4]. From the analysis, the GF shaft moved largely after contacting with snare wire and vibrated in enclosed region just before fixed by snare wires. In this section, we executed four experiments with different initial conditions. The first experiment was executed under the same condition of the reference [4] to evaluate the performance of the HMS. The other three experiments were executed with different initial velocity and angular velocity for case study.

5.1 Experimental Condition

An overview of the experiment system is shown in Fig. 10. The GF was mounted on the HEXA, and the LEE was mounted on the flame. The HEXA demonstrated the relative motion between LEE and GF because the LEE was fixed at the flame. In the experiments, the GF shaft was assumed to be inside the enclosed region formed by snare wires in the initial condition.

The numerical models of the SSRMS and the HTV were designed as the half-scaled model by following the similarity rule mentioned in Section 3. The experimental conditions are listed in Table 2. The 1st condition was almost same as the condition of reference [4]. The 2nd

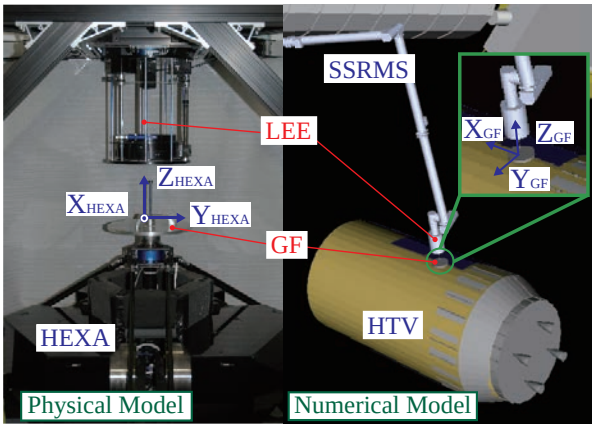

Figure 10. Overview of the HMS for HTV mission

Table 2. Experimental conditions

Condition	V_x [mm/s]	V_y [mm/s]	W_{roll} [°/s]	W_{pitch} [°/s]
1 (same as in [4])	-0.0033	0.0035	-0.32	0.3
2	0	15	0	0
3	0	30	0	0
4	0	30	0.2	0

condition was set to be the maximum allowed relative velocity in the real orbital HTV mission. The 3rd and 4th conditions were set to be over the maximum allowed relative velocity and angular velocity in the real orbital HTV mission. In the real scaled operation, the maximum allowed relative velocity is about 30 [mm/s]. The relative velocity applied to the HMS was also scaled down by following the rule of similarity as shown in Table 2.

5.2 Experimental Results and Discussion

With the first condition, the HTV in the HMS behaved with almost same characteristic as the reference [4]. Fig. 11 shows sequential snapshots of the simulator for capturing the HTV in the 2nd condition. The results of 2nd, 3rd and 4th conditions are shown in Fig. 12 to 15, respectively. It was observed from the relative positions X_{HEXA} and Y_{HEXA} that the GF shaft moved largely with a few times bouncing motion while contacting with the snare wires. The relative attitudes *Roll* and *Pitch* were increasing. This characteristic occurred because step 4 in Fig. 2 was not executed in the experiments. The relative position Z_{HEXA} in each condition increased because the HTV went away from the envelope of the LEE. This was also because the torque T_X occurred on the tip of the GF and the HTV moved toward the direction of GF leaving the LEE rotating. The forces F_X and F_Y were discontinuous from each force graph. This was because the enclosed region made by snare wires became loose a little. Therefore, the GF shaft was moving a little inside the enclosed

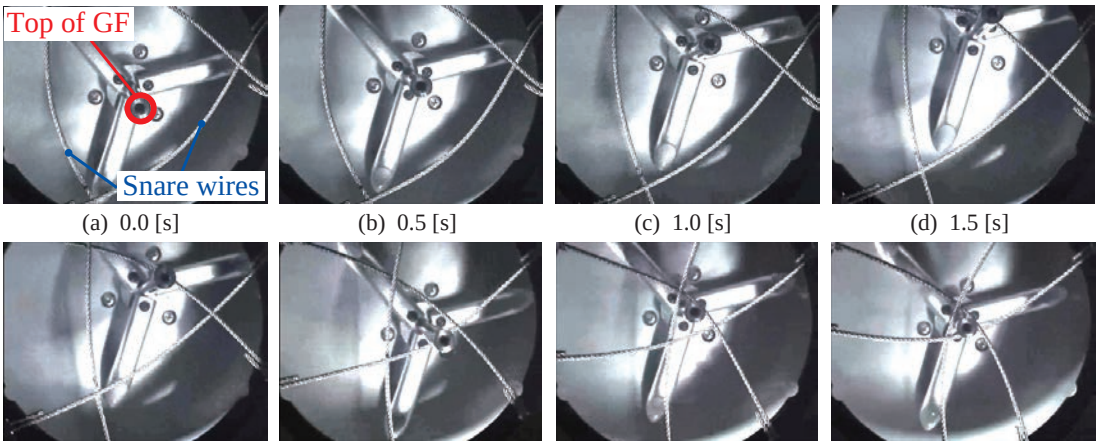

(a) 0.0 [s] (b) 0.5 [s] (c) 1.0 [s] (d) 1.5 [s]

(e) 2.0 [s] (f) 3.0 [s] (g) 4.0 [s] (h) 6.0 [s]

Figure 11. Sequential photographs of the simulation for capturing HTV

region.

Here, we compare the relative behaviors among the experimental conditions. First, we discuss the results of 2nd and 3rd conditions. The difference between 2nd and 3rd conditions was the velocity. The velocity in the 2nd condition was 15 [mm/s] which was almost equal to the limited velocity in the real orbital HTV mission. The velocity in the 3rd condition was 30 [mm/s] which was twice faster than the limited velocity. It was found from the results that the force of first contact and displacement magnitude of Z_{HEXA} were larger when the initial velocity increased. This was because the impact increased and the larger force and torque occurred in the direction of leaving.

Next, we discuss the results of 3rd and 4th conditions. The difference between 3rd and 4th conditions was the angular velocity. There was no initial angular velocity in the 3rd condition while the angular velocity in the 4th condition was set to be 0.2 $[^\circ/s]$ which was about twice value of the limited angular velocity in the real orbital HTV mission. It was observed from the results that the angular velocity affected the relative attitude largely. On the other hand, the angular velocity did not affect the force and torque. The capture succeeded under the twice value of the limited velocity and angular velocity. However the limit of angular velocity cannot exceed largely because there is a possibility of accidental crash between LEE and GF before step 4 in Fig. 2 is finished.

From the above case study, the simulator can evaluate the HTV capture operation over the allowed condition for the safety. Furthermore, it is confirmed that the simulator is useful to evaluate safe grasping method for unexpected accidental contact.

6 Conclusions

This paper described the development of a hybrid motion simulator for capturing the HTV by the flexible space manipulator, SSRMS. The half-scaled mockups of LEE and GF were developed for capturing mechanism in the hardware experiment in the HMS. The entire dynamic models of the SSRMS and HTV were constructed in the numerical simulator. Due to the scaled hardware mockups, the dynamic models were scaled down by following the similarity rule between real and numerical models. The derived similarity rule was verified with simple articulated body system. In order to evaluate the stability of the HMS system for capturing the HTV, we carried out the frequency analysis of the contact dynamics and analyzed the COR. Case study was executed with the developed HMS, and it was observed from the results that the simulator could present the characteristic of the real grasping motion of the GF by the LEE.

In the future, this simulator will be useful for checking new method for capturing the massive payload by using LEE and GF mechanism. Furthermore, this simulator will be also efficient for proposing avoiding method when the unforeseen accident occurs.

Acknowledgment

This research is a part of a collaboration work between Tohoku University and Japan Aerospace Exploration Agency (JAXA).

References

[1] H. Ise et al. : “Development of a 9-DOF Hybrid Motion Simulator for Simulating Motion under Micro-Gravity Environment,” *in Proc. of the 24th Annual Conference of the Robotics Society of Japan*, 2006 (in Japanese).

[2] N. Uyama et al. : “Analysis on Contact Dynamics Between LEE (Latching End Effector) of Space Station Remote Manipulator System and a Floating Target,” *in Proc. of 18th workshop on JAXA Astrodynamics and flight mechanics*, 2008.

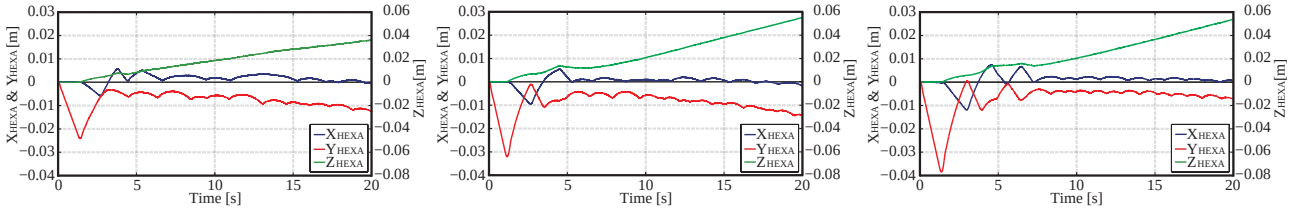

(a) V_y = 15 [mm/s] (b) V_y = 30 [mm/s] (c) V_y = 30 [mm/s] and W_{roll} = 0.2 [°/s]

Figure 12. Result of relative position at each initial condition

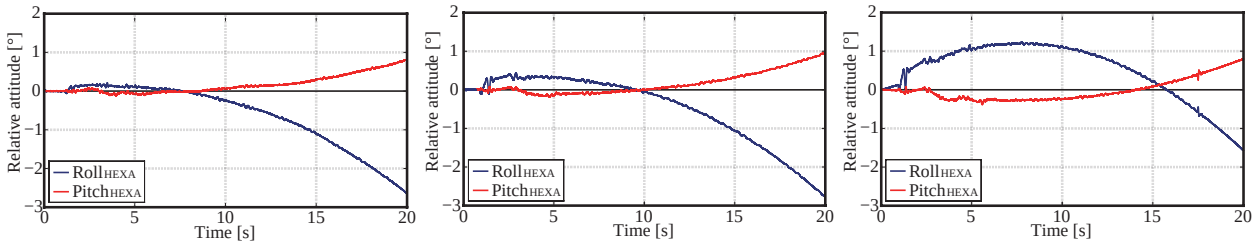

(a) V_y = 15 [mm/s] (b) V_y = 30 [mm/s] (c) V_y = 30 [mm/s], W_{roll} = 0.2 [°/s]

Figure 13. Result of relative attitude at each initial condition

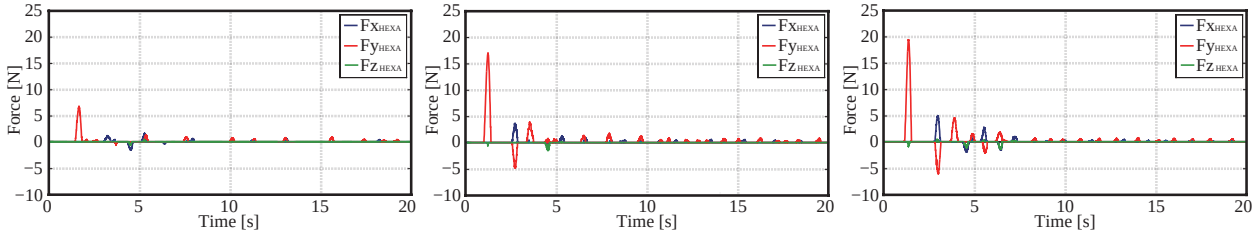

(a) V_y = 15 [mm/s] (b) V_y = 30 [mm/s] (c) V_y = 30 [mm/s], W_{roll} = 0.2 [°/s]

Figure 14. Result of force of GF at each initial condition

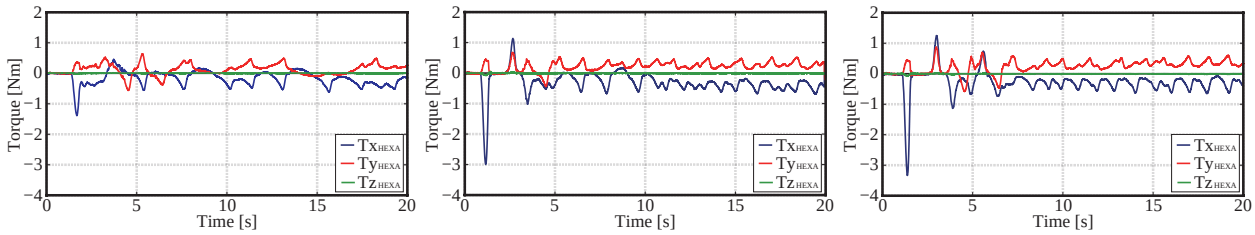

(a) V_y = 15 [mm/s] (b) V_y = 30 [mm/s] (c) V_y = 30 [mm/s], W_{roll} = 0.2 [°/s]

Figure 15. Result of torque of GF at each initial condition

[3] S. Abiko et al. : "Contact Dynamics Simulation for Capture Operation by Snare Wire Type of End Effector," *in Proc. of the 11th i-SAIRAS*, 03B-02, 2012.

[4] H. Nakanishi et al. : "The Motion Analysis of the HTV Capture with the Space Station Remote Manipulator System (SSRMS)," *in Proc. of JSME Robotics and Mechatronics Conference*, 2012 (in Japanese).

[5] P. K. Nguyen et al. : "Teleoperation: From the Space Shuttle to the Space Station," *AIAA Progress in Astronautics and Aeronautics*, vol. 161, pp. 353–410, 1994.

[6] H. Ueno : "On-orbit Characteristics of Kibo Robot Arm," *in Proc. of 54th Space Sciences and Technology Conference*, 2010 (in Japanese).

[7] I.Takahashi et al. : "Development of Hybrid Motion Simulator for Capturing H-II Transfer Vehicle," to be published in *Journal of The Japan Society for Aeronautical and Sciences* (in Japanese).

[8] K. Osaki et al. : "Delay Time Compensation for a Hybrid Simulator," *Advanced Robotics*, vol. 24, no. 8–9, pp. 1081–1098, 2010.